Human Molecular Genetics, 2003, Vol. 12, No. 10 **1145–1154**
DOI: 10.1093/hmg/ddg126

A very long-chain acyl-CoA synthetase-deficient mouse and its relevance to X-linked adrenoleukodystrophy

Ann K. Heinzer[1,2,4], Paul A. Watkins[1,3], Jyh-Feng Lu[5], Stephan Kemp[6], Ann B. Moser[1], Yuan Yuan Li[1], Stephanie Mihalik[1], James M. Powers[7] and Kirby D. Smith[1,2,4,*]

[1]The Kennedy Krieger Institute, [2]Department of Pediatrics, [3]Department of Neurology and [4]Institute of Genetic Medicine, The Johns Hopkins School of Medicine, Baltimore, MD 21205, USA, [5]Fu Jen Catholic University, School of Medicine, Hsinchung Hsih, Taipei Hsien, Taiwan, Republic of China, [6]Laboratory of Genetic Metabolic Diseases, Emma Children's Hospital, Academic Medical Center, University of Amsterdam, 1105 AZ Amsterdam, The Netherlands and [7]Departments of Pathology and Laboratory Medicine, University of Rochester Medical Center, Rochester, NY 14642, USA

Received January 7, 2003; Revised and Accepted March 14, 2003

X-linked adrenoleukodystrophy (X-ALD) is a neurodegenerative and endocrine disorder resulting from mutations in *ABCD1* which encodes a peroxisomal membrane protein in the ATP binding cassette superfamily. The biochemical signature of X-ALD is increased levels of saturated very long-chain fatty acids (VLCFA; carbon chains of 22 or more) in tissues and plasma that has been associated with decreased peroxisomal very long-chain acyl-CoA synthetase (VLCS) activity and decreased peroxisomal VLCFA β-oxidation. It has been hypothesized that ABCD1, which has no demonstrable VLCS activity itself, has an indirect effect on peroxisomal VLCS activity and VLCFA β-oxidation by transporting fatty acid substrates, VLCS protein or some required co-factor into peroxisomes. Here we report the characterization of a Vlcs knockout mouse that exhibits decreased peroxisomal VLCS activity and VLCFA β-oxidation but does not accumulate VLCFA. The XALD/Vlcs double knockout mouse has the biochemical abnormalities observed in the individual knockout mice but does not display a more severe X-ALD phenotype. These data lead us to conclude that (1) VLCFA levels are independent of peroxisomal fatty acid β-oxidation, (2) there is no ABCD1/VLCS interaction and (3) the common severe forms of X-ALD cannot be modeled by decreasing peroxisomal VLCS activity in the XALD mouse.

INTRODUCTION

X-linked adrenoleukodystrophy (X-ALD) is a neurodegenerative disorder that also affects testis and adrenal glands and is diagnosed by elevated amounts of saturated straight chain very-long-chain fatty acids (VLCFA; fatty acids with 22 or more carbons) in patient plasma (1). This characteristic VLCFA accumulation is accompanied by a diminished ability to degrade VLCFA via peroxisomal β-oxidation as observed in patient fibroblasts (2–5). VLCFA are degraded exclusively by peroxisomal β-oxidation. The first enzymatic step in VLCFA β-oxidation, the activation of VLCFA to their CoA derivatives, is encoded by the enzyme very long-chain acyl-CoA synthetase, VLCS. This enzymatic activity is decreased in peroxisomes from fibroblasts of X-ALD patients and has been implicated as the cause of the decrease in VLCFA β-oxidation and VLCFA accumulation (6–8).

The X-ALD gene, *ABCD1*, encodes a peroxisomal membrane half-ABC transporter, ABCD1 (or ALDP) (9). The function of ABCD1 is unknown, but its similarity to membrane transport proteins and the lack of any measurable VLCS activity makes it unlikely that ABCD1 encodes a peroxisomal VLCS. ABCD1 cannot therefore be directly responsible for the X-ALD enzymatic defect (decreased peroxisomal VLCS activity in fibroblasts); however, overexpression of *ABCD1* cDNA in XALD fibroblasts increases VLCFA β-oxidation and reduces VLCFA accumulation (10–12). It has been proposed that ABCD1 transports VLCFA, VLCS enzyme, or

*To whom correspondence should be addressed at: RM 400A Kennedy Krieger Institute, 707 North Broadway, Baltimore, MD 21205, USA. Tel: +1 4439232751; Fax: +1 4439232775; Email: smithk@jhmi.edu

a required cofactor across the peroxisomal membrane and thereby controls peroxisomal VLCS activity, VLCFA β-oxidation and VLCFA levels.

An enzyme with VLCS activity was first isolated from rat liver peroxisomes in 1995 (13) and the gene encoding this enzyme was cloned in 1996 (14). In *S. cerevisiae*, strains lacking a VLCS ortholog, FAT1, have decreased VLCFA β-oxidation and accumulate VLCFA mimicking X-ALD fibroblasts (15). A family of related mammalian genes was subsequently found that includes fatty acid transport protein (FATP) and bile acyl-CoA synthetase (15–21). Several of these genes encode enzymes with some VLCS activity but the human and mouse orthologs of the original rat VLCS (human VLCS and mouse Vlcs) are the only mammalian VLCS proteins with a documented peroxisomal localization (22,23) and could thereby participate in VLCFA β-oxidation. A possible role for mouse Vlcs in VLCFA β-oxidation is suggested by the observation that its overexpression increases VLCFA β-oxidation in X-ALD fibroblasts (23) but the relationship between Abcd1 and Vlcs is still unknown.

The *Abcd1* knockout mouse (XALD mouse) mimics the human biochemical profile, i.e. accumulation of VLCFA in tissues and decreased VLCFA β-oxidation in fibroblasts (24–26). XALD mice have adrenal dysfunction but do not display a neurological phenotype until 18–20 months of age when a very mild neuropathy manifests similar to adrenomyeloneuropathy (AMN) (27), a late-onset, slower progressing X-ALD phenotype that effects ∼40% of all X-ALD patients (28). These mice do not have a severe inflammatory demyelination analogous to that seen in childhood cerebral X-ALD, which affects another 40% of X-ALD patients.

We have recently demonstrated that peroxisomal Vlcs protein levels are unchanged and that peroxisomal VLCS activity is normal in XALD mouse liver. Most surprisingly, we have shown that VLCFA β-oxidation in XALD mouse tissues is also normal (23,29). These observations are inconsistent with hypotheses that arose from observations of human X-ALD fibroblasts which suggested that ABCD1 mediates peroxisomal Vlcs localization, activity or expression. They also indicate that the VLCFA accumulation seen in XALD is not a result of their decreased degradation by peroxisomal β-oxidation and that ABCD1 is not a direct participant in peroxisomal VLCFA β-oxidation. A hypothesis to explain the discrepancy between XALD fibroblasts and XALD tissue VLCFA β-oxidation has been proposed in another paper that investigates fibroblast VLCFA β-oxidation and mitochondrial function (29).

These observations raise the following questions: (1) does the XALD mouse fail to develop a severe X-ALD phenotype because it does not replicate the metabolic deficiencies of peroxisomal VLCS activity and VLCFA β-oxidation as observed in X-ALD patient fibroblasts? (2) If these biochemical abnormalities are replicated in mouse tissues what effect will they have on VLCFA levels? That is, are VLCFA levels controlled by VLCFA degradation?

In order to answer these questions, we first generate and characterize a Vlcs knockout mouse. Second, we replicate the biochemical abnormality observed in X-ALD human fibroblasts through the generation of a Vlcs knockout mouse and an XALD/Vlcs double knockout mouse. We report ability of both these models to activate, β-oxidize, and accumulate VLCFA; and observe these mice for signs of a severe, early-onset, neurodegenerative X-ALD phenotype.

RESULTS

Vlcs is disrupted in mouse embryonic stem cells

Embryonic stem cells (ES cells) from 129Svev embryos were transfected with a knockout construct that replaces 69 bp of Vlcs exon 3 with a 1100 bp neomycin-resistance cassette and selected for resistance to neomycin (Fig. 1A). The knockout construct encompasses 7 kb and is composed of *Vlcs* exon 2, intron 2, a neomycin-resistance cassette in place of most of *Vlcs* exon 3, intron 3 and exon 4. The introduction of the neomycin-resistance cassette increases the size of a Hind III genomic DNA fragment detected by a probe outside of exon 2 from 6 to 7 kb (Fig. 1B).

Resistant ES cell colonies were cultured and screened for homologous recombination of the construct with the *Vlcs* locus by Southern blot analysis of ES cell clone genomic DNA (Fig. 1B). Four ES cell clones out of 579 screened underwent single homologous recombination events. Of these four ES cell clones, three had normal karyotypes (data not shown) and were used for injection into mouse blastocysts. Two produced a total of six chimeric mice that transmitted the disrupted allele through the germline. Germline chimeras were identified by producing agouti-colored progeny when mated to C57BL/6 mice.

Vlcs mice are viable and fertile

Germline-transmitting chimeras were crossed to wild-type 129Svev females to establish a Vlcs mouse line. The heterozygous progeny were verified by Southern blot analysis. These mice were fertile and produced litters containing wild-type, heterozygous and homozygous Vlcs mice (hereafter referred to as Vlcs mice). Vlcs mice are also fertile and true-breeding lines were generated by brother/sister matings. Lines were generated from two independent homozygous recombinant ES cell clones and mice from each line were similar in all aspects examined (data not shown).

Vlcs mice are morphologically unchanged

Vlcs mice do not have any apparent gross morphological abnormalities and are indistinguishable from wild type or heterozygous littermates. Observations of routine behaviors, feeding, sleeping and mobility did not indicate any abnormalities and gross examination of internal organs did not reveal any malformations (data not shown).

A histological examination of Vlcs mouse liver, brain and kidney indicated that there are no significant histological changes in these tissues as a result of Vlcs gene disruption (Fig. 2).

Vlcs mice do not express Vlcs protein

Successful generation of a Vlcs mouse was confirmed by a combination of methods including southern blot, PCR and western blot analyses. No wild-type alleles were detected in the

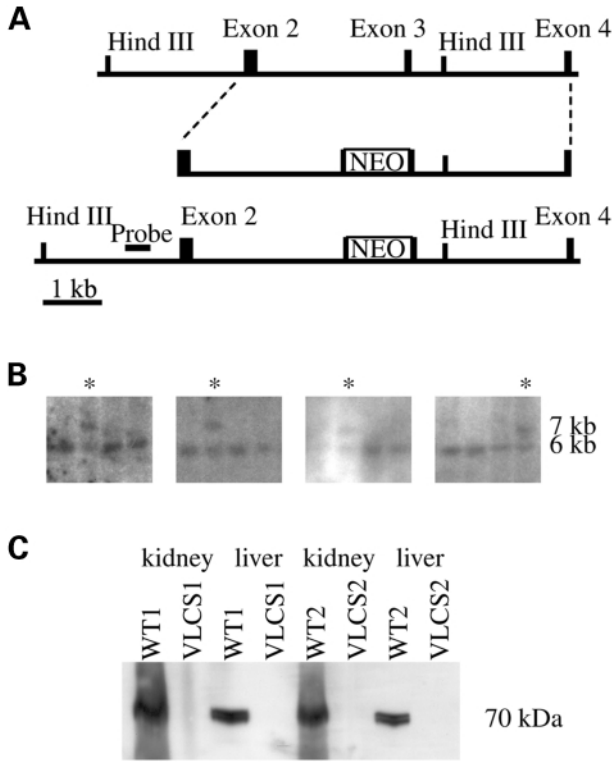

Figure 1. The *Vlcs* disruption construct, screen for ES cell clones with homologous recombinations, and test of Vlcs expression in Vlcs mouse tissues. (**A**) A diagram of the disrupted segment of the mouse *Vlcs* gene. The wild-type allele is shown above the recombined knockout allele. Boxes indicate exons 3, 4 and 5, and a disruption cassette containing a neomycin resistance gene behind its promoter (NEO). The *Hind*III sites used for the southern blot screen of ES cells are also shown. The horizontal bold line to the left of exon 2 indicates the nucleotide sequences used as a radiolabeled probe in the screen. A 1 kb bar at the bottom of (A) indicates the scale. Homologous recombination of the knockout construct at the *Vlcs* locus increases the size of the recombined knockout genomic DNA *Hind*III fragment from 6 to 7 kb. (**B**) The results of a southern blot analysis of DNA from neomycin resistant ES cell clones. DNA from these clones was restricted with *Hind*III, transferred to nylon and detected with the DNA probe indicated in (A). The 1 kb increase in size of the *Hind*III fragment from 6 to 7 kb predicted from the homologous recombination of the construct can be seen in the four clones marked with an asterisk. Homologously recombined clones also have a 6 kb wild-type allele and clones that have non-homologous recombinations have only the 6 kb wild-type allele. (**C**) Western blot analyses of liver and kidney tissue extracts from two adult mice homozygous for the *Vlcs* gene disruption (Vlcs 1 and Vlcs 2) and two mice with normal *Vlcs* genes (WT 1 and WT 2). A doublet is detected in wild-type kidney (lanes 1 and 5) and liver (lanes 3 and 7) near 70 kDa, but not in kidney and liver from homozygous *Vlcs* mice (lanes 2, 6 and lanes 4, 8). Each lane has the same amount of total protein (80 μg) as determined by the Lowry method and the blot was exposed for 30 s.

Vlcs mouse by Southern blot analyses or PCR (data not shown) and Vlcs protein is not detectable in Vlcs mouse liver, kidney, brain or adrenal gland homogenates (Fig. 1C and 3B) using an affinity-purified antibody specific for mouse Vlcs protein (see Methods). The blot in Figure 3B was overexposed in order to reveal the small amount of Vlcs protein in mouse adrenal gland. As previously noted (23), Vlcs protein is detected as a doublet in wild-type tissues. Both protein species are absent in the Vlcs mouse indicating that they are both the product of the *Vlcs* gene.

VLCS activity is decreased in liver and kidney of the Vlcs mouse

A reduction in VLCS activity was observed in the liver and kidney post-nuclear supernatants of Vlcs mice but not in brain or adrenal glands (Fig. 3A). The latter are important sites of X-ALD pathology. In agreement with previously published data, Vlcs is highly expressed in liver and kidney with lesser but detectable amounts of message in brain, heart, muscle and adrenal glands of wild-type mice. VLCS activity is reduced most dramatically in the Vlcs mouse liver and kidney with a 4-fold reduction in liver and a 9-fold reduction in kidney. VLCS activity was unchanged in brain and adrenal glands. The residual activity remaining in liver and kidney and the unchanged levels in brain and adrenal glands indicates that other VLCS enzymes exist in these tissues.

VLCS activity is decreased in Vlcs mouse liver peroxisomes and microsomes

Vlcs protein and activity are present in both peroxisomes and microsomes (23). PEX 14, a peroxisomal membrane protein, was used to identify peroxisome-containing fractions from mouse liver density fractionation in Figure 4. Fractions 1/2 contained the majority of PEX14 with some in fractions 3/4 and none in any other fractions. Microsomal fractions were identified as those containing calreticulin, an ER protein, and consisted of fractions 7/8 to 17/18. The majority of Vlcs protein and general VLCS activity is found in microsomal fractions (Fig. 4). As expected, Vlcs protein is lost from both peroxisomal and microsomal liver fractions in the Vlcs mouse (Fig. 4B) and VLCS activity is decreased in both peroxisomal and microsomal fractions (Fig. 4A). Both microsomal and peroxisomal fractions retain similar amounts of residual VLCS activity (30% of wild-type). This suggests that *Vlcs* encodes an enzyme that is responsible for the majority of VLCS activity in the peroxisomes and microsomes of both liver and kidney, tissues with relatively more VLCS activity than other tissues (see Fig. 3A). VLCS is not the only very long-chain acyl-CoA synthetase enzyme in either one of these compartments as residual VLCS activity is detected in both these compartments in the Vlcs mouse.

VLCFA β-oxidation is reduced in Vlcs mouse tissues

The small fraction of cellular VLCS activity that resides in the peroxisome is decreased in X-ALD patient fibroblasts. This localized decrease has been hypothesized to cause the decreased peroxisomal VLCFA β-oxidation and VLCFA accumulation that is seen in these patient cell lines. Fibroblasts from XALD mice also have decreased levels of VLCFA β-oxidation and accumulate VLCFA. Since XALD mouse tissues, as well as fibroblasts, accumulate VLCFA it had been assumed that XALD mouse tissues also have a VLCFA β-oxidation defect. We have recently reported that all XALD mouse tissues examined (excluding cultured fibroblasts) possess normal levels of VLCFA β-oxidation activity (29) and VLCS activity (23), and that XALD mouse liver peroxisomes have normal amounts of Vlcs protein and VLCS activity (23). These observations challenge current

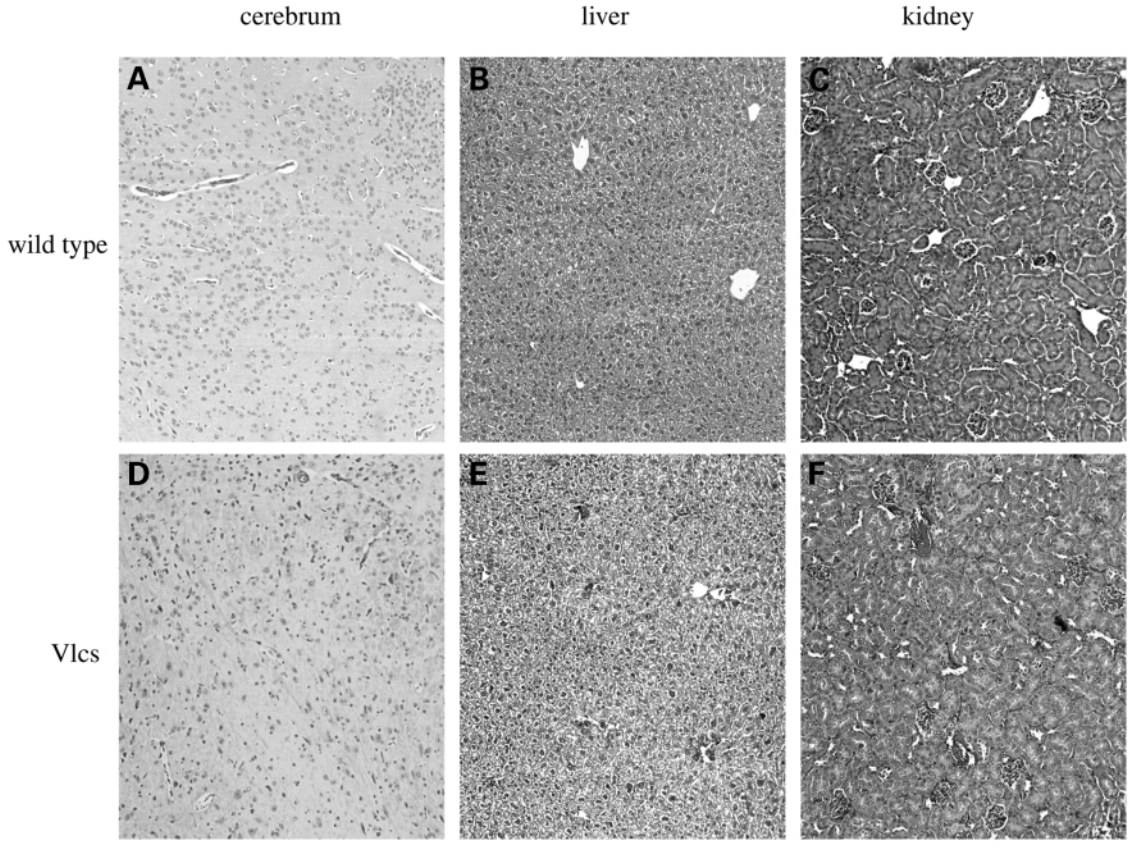

Figure 2. Vlcs mouse tissue morphology is unchanged. H&E stained tissue sections from wild type and Vlcs mouse cerebrum, liver and kidney are shown at 400× magnification. (**A**–**C**) Wild-type cerebrum, liver and kidney respectively; and (**D**–**F**) Vlcs cerebrum, liver and kidney, respectively. These images are representative of six male mice examined from each genotype at 8 weeks of age.

explanations for VLCFA accumulation in X-ALD. The Vlcs mouse has decreased peroxisomal VLCS activity (Fig. 4A) and if the current explanation is correct then the Vlcs mouse should have decreased peroxisomal VLCFA β-oxidation and VLCFA accumulation as a result.

We find that VLCFA β-oxidation in the Vlcs mouse is indeed decreased in those tissues where significant VLCS activity is lost, i.e. liver and kidney, but find no effect on the VLCFA β-oxidation levels in brain (Fig. 5A). As in X-ALD fibroblasts, Vlcs mouse VLCFA β-oxidation is not eliminated but is decreased. In the mouse, VLCFA β-oxidation is decreased to ∼40% of normal levels (from 1.5 to 0.65 C24:0 nmol/h/mg protein in liver and from 2.2 to 1.0 C24:0 nmol/h/mg protein in kidney).

Despite this decrease in VLCFA degradation VLCFA do not accumulate in Vlcs mouse tissues (Fig. 5B). Levels of C26:0 are unchanged in brain and kidney tissues from the Vlcs mouse. Liver levels are not increased and may be slightly decreased (from 0.02 to 0.01 C26:0/C22:0 with overlapping standard deviations). When these data are expressed as total micrograms of C26 per mg of tissue protein, the same results are obtained (data not shown).

Thus, the association in human XALD fibroblasts between VLCFA accumulation, decreased peroxisomal VLCS activity and decreased VLCFA β-oxidation is not replicated in the XALD mouse or in the Vlcs mouse. A mouse with the combined biochemical abnormalities of both mice may better model X-ALD; therefore, we generated an XALD/Vlcs double knockout mouse. This mouse will further assess any Abcd1/Vlcs interaction.

Construction and gross morphology of XALD/Vlcs mice

We crossed homozygous XALD females and homozygous Vlcs males through two generations to generate XALD/Vlcs double knockout mice. Heterozygotes, hemizygotes and double homozygotes were observed in the expected ratios. Interbred XALD/Vlcs mice produced normal-sized, healthy litters. Thus, the combined loss of Abcd1 and Vlcs does not affect embryonic viability or result in any obvious morphological defect at birth. No outward defects were observed in the double knockout mice; they were indistinguishable from wild-type mice and displayed no signs of abnormality through 1 year of age.

VLCS activity is reduced in XALD/Vlcs mice to the same levels as in Vlcs mice

VLCS activity is decreased in the XALD/Vlcs mouse, but not more than in the Vlcs mouse (Fig. 6A). Vlcs activity in liver, brain and kidney from wild-type, XALD, Vlcs and XALD/Vlcs

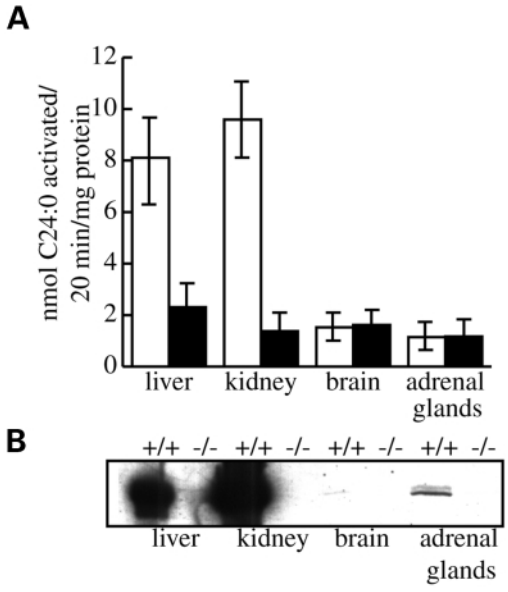

Figure 3. VLCS activity is significantly reduced in Vlcs mouse liver and kidney. (**A**) Homogenates from wild-type (open bars) and Vlcs (solid bars) mouse tissues that were assayed for VLCS activity using radiolabeled C24:0 as a substrate. Error bars indicate ±1 SD from the mean of at lease three separate measurements in tissues from at least three individual mice assayed in duplicate. (**B**) Western blot analysis of these wild-type and Vlcs mouse tissues for Vlcs protein. The blot was overexposed (5 min) to highlight the Vlcs protein in wild type brain and adrenal glands.

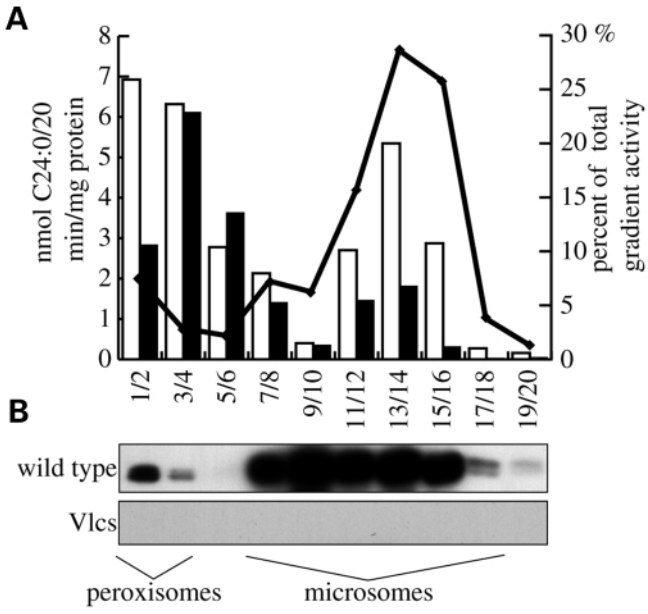

Figure 4. VLCS activity and Vlcs protein are lost from both peroxisomes and microsomes in Vlcs mouse liver. (**A**) Liver homogenates from wild-type and Vlcs mice fractionated on 30 ml Nycodenz density gradients. Twenty fractions (2 ml each) were collected and assayed for VLCS activity and protein concentration. Equal volume samples from each fraction were subjected to gel electrophoresis, transferred to a membrane and probed with a mouse Vlcs-specific antibody. In the top panel, VLCS specific activity from wild type (open bars) and Vlcs (solid bars) liver are indicated. A line (solid diamonds) indicates the percentage of total VLCS activity in the gradient per fraction. (**B**) Western blots of the same wild type (top) and Vlcs (bottom) mouse liver fractions. Fractions containing peroxisomes and microsomes are indicated. These fractions were determined using organelle specific marker antibodies, anti-PEX14 for peroxisomes and anti-calreticulin for microsomes. The blot was exposed for 30 s.

mice was measured using a representative very long-chain fatty acid, lignoceric acid (C24:0), and each measurement is the average of duplicate assays from at least three individual mice.

In the Vlcs mouse, VLCS activity is decreased in liver and kidney, from about 5.8 to 1.5 nmol C24/20 min/mg protein in both tissues whereas VLCS activity in brain remains unchanged at 1.2 nmol C24/20 min/mg protein. XALD/Vlcs mouse tissues have a similar decrease in VLCS activity from 8 to 2 or 1.2 nmol C24/20 min/mg protein in the same tissues seen in the Vlcs mouse, but not more. Therefore, the lack of Abcd1 does not have any effect on the tissue location or the magnitude of VLCS activity in these mice.

The decrease in VLCFA β-oxidation seen in Vlcs mice is not augmented in XALD/Vlcs mice

As previously described, XALD mouse tissue VLCFA β-oxidation levels are unchanged from wild-type levels in liver (1.5 and 1.6 nmol C24/h/mg protein), brain (0.15 and 0.2) and kidney (2.2 and 2.0) (29). Vlcs mouse VLCFA β-oxidation levels are half of wild-type levels in liver and kidney, from 1.5 units to 0.7 units in liver and from 2.2 units to 1.0 units in kidney, while adrenal gland and brain levels are unchanged at 0.2 units each (Fig. 6B).

The amount of XALD/Vlcs tissue VLCFA β-oxidation activity matches that of Vlcs mouse tissues with 0.8 units in liver, 0.2 units in brain, and 0.8 units in kidney. XALD/Vlcs mice have the same tissue VLCFA β-oxidation activity in tissues as the Vlcs mouse; thus, a lack of Abcd1 does not worsen or correct the VLCFA β-oxidation defect seen in the Vlcs mouse.

VLCFA levels in the XALD/Vlcs mouse are not elevated more than XALD mouse VLCFA levels

VLCFA levels in the XALD/Vlcs mouse are the same as in the XALD mouse (Fig. 6C). The C26/C22 ratio is reported in tissues from wild-type, XALD, Vlcs and XALD/Vlcs mice. As previously observed, XALD mouse tissues have increased C26:0 levels in liver, brain and kidneys (2.5–3-fold over wild-type levels). VLCFA levels in Vlcs mice are not increased, even though a defect in VLCFA β-oxidation is observed in these mice. The combination of these two genetic defects in one mouse, the XALD/Vlcs mouse, does not increase the VLCFA levels beyond XALD mouse levels. Tissue C26/C22 ratios are identical to ratios in XALD mouse tissues and are not normalized or increased (0.05 in liver, 0.15 in brain and 0.15 in kidney). Levels of other chain length fatty acids were also assayed and no significant accumulations or deficiencies were observed in the Vlcs or the XALD/Vlcs mice.

DISCUSSION

Vlcs mice have a normal gross and neurological phenotype even though they lack Vlcs expression. In the Vlcs mouse, Vlcs protein is not detected by western blot in any tissue and VLCS activity is dramatically decreased in liver and kidney (Fig. 3A).

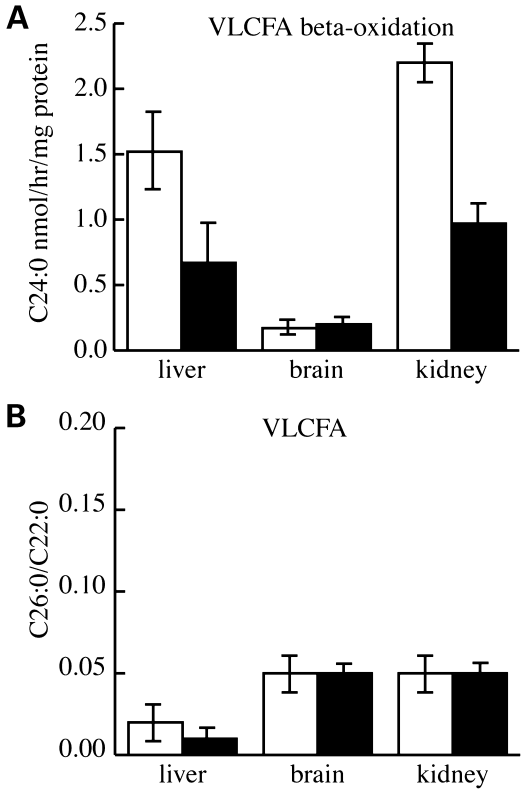

Figure 5. Saturated VLCFA β-oxidation is decreased, but VLCFA levels are unchanged in Vlcs mouse tissues. (**A**) VLCFA β-oxidation activity in tissues from wild-type (open bars) and Vlcs mice (solid bars). Liver, brain and kidney extracts from 8-week-old mice were assayed for their ability to perform at least one round of β-oxidation on radiolabeled lignoceric acid (C24:0). VLCFA β-oxidation specific activity is expressed as the average of three or more measurements made in duplicate. (**B**) VLCFA levels in tissues from wild-type (open bars) and Vlcs (solids bars) mice. Liver, brain and kidneys were harvested from 8-week-old mice and homogenized in solvent. Lipids were extracted and derivatized to their methyl esters which were separated by gas chromatography and quantified by comparing to known standards. This data is expressed as the ratio of C26:0 (cerotic acid) to C22:0 (behenic acid). Error bars indicate ±1 SD from the average of three different animals per genotype assayed in duplicate.

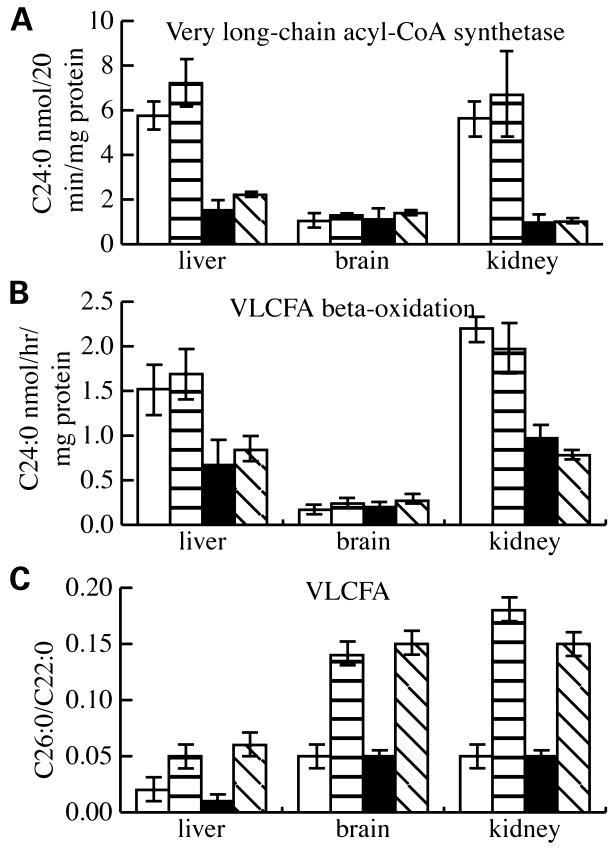

Figure 6. Vlcs activity, VLCFA β-oxidation and VLCFA accumulation are not synergistically increased or decreased in XALD/Vlcs double knockout mice. (**A**) VLCS activity in tissues from wild-type (open bars), XALD (bars with horizontal lines), Vlcs (Solid bars) and XALD/Vlcs mice (hashed bars). Liver, brain and kidney extracts from 8-week-old mice were assayed for their ability to activate lignoceric acid (C24:0) to its CoA derivative. (**B**) VLCFA β-oxidation activity in tissues from wild-type (open bars), XALD (bars with horizontal lines), Vlcs (solid bars) and XALD/Vlcs mice (hashed bars). Liver, brain and kidney extracts from 8-week-old mice were assayed for their ability to perform β-oxidation on radiolabeled lignoceric acid (C24:0). These are the same tissue extracts in which VLCS activity was measured for Figure 5. (**C**) VLCFA levels in tissues from wild type (open bars), XALD (bars with horizontal lines), Vlcs (solid bars) and XALD/Vlcs mice (hashed bars). Liver, brain and kidneys were harvested from 8-week-old mice and homogenized in solvent. Lipids were extracted and derivatized to their methyl esters which were separated by gas chromatography and quantified by comparing with known standards. This data is expressed as the ratio of C26:0 (cerotic acid) to C22:0 (behenic acid). Error bars indicate ±1 SD from the average of three different animals per genotype assayed in duplicate.

VLCS activity is unchanged in brain and adrenal glands, where Vlcs is not highly expressed in the wild-type mouse which suggests that other VLCS enzymes are responsible for the activity in these tissues. In addition, residual activity remaining in liver and kidney implies that other VLCS enzymes are present there as well. This activity may be encoded by recently identified VLCS-like enzymes such as Fatp1, Fatp4 or bubblegum (lipidosin), and one of these or some unidentified VLCS enzyme may also be responsible for the majority of VLCS activity in brain and adrenal glands.

Prior to recent publications (23,30) the accepted biochemical model of X-ALD attributed VLCFA accumulation in all tissues to defects in peroxisomal VLCS activity and VLCFA degradation. These defects were hypothesized to result from a faulty interaction between Abcd1 and a peroxisomal VLCS enzyme. Therefore, any tissue that accumulates VLCFA in X-ALD should demonstrate the metabolic defects that result from this faulty interaction. Although Vlcs is not highly expressed in tissues affected pathologically in X-ALD—brain and adrenal glands—and VLCS activity is not reduced in these tissues in the Vlcs mouse, an examination in liver of the interaction between Abcd1 and Vlcs is relevant since liver (and all other tissues examined) accumulate VLCFA in X-ALD.

The Vlcs mouse has decreased VLCS activity and VLCFA β-oxidation in liver peroxisomes and thus replicates the presumed metabolic defect seen in X-ALD patient fibroblasts. Both peroxisomal and microsomal compartments lose most of their VLCS activity in the Vlcs mouse liver indicating that Vlcs accounts for the majority of activity in both compartments (Fig. 4A). Vlcs also appears to be the primary VLCS enzyme for VLCFA β-oxidation in liver and kidney as 60–80% of VLCS activity is lost and there is a 50–60% reduction in

VLCFA β-oxidation activity in these tissues (Fig. 5A). Yet, Vlcs is not essential for VLCFA β-oxidation as it is not completely absent from these tissues. Interestingly, VLCFA β-oxidation is not completely lost from X-ALD fibroblasts either. They retain ∼30% of normal activity even in lines with null *ABCD1* alleles (2,3). The Vlcs mouse shows that the previous biochemical model for X-ALD is partly correct—decreased but not absent peroxisomal VLCS activity results in decreased but not absent VLCFA β-oxidation activity. It is clear that peroxisomal Vlcs has a role in VLCFA β-oxidation but observations of the Vlcs mouse have not yet enlightened us about what metabolic pathways require microsomal Vlcs.

In contrast to fibroblasts from X-ALD patients, the Vlcs mouse's decreased ability to degrade VLCFA via peroxisomal β-oxidation is not associated with increased VLCFA in tissues (Fig. 5B). This observation does not support the previous biochemical model of X-ALD whereby VLCFA accumulate as a result of a VLCFA β-oxidation defect. Recently, we showed that the XALD mouse has normal VLCFA β-oxidation, normal peroxisomal VLCS activity and localization, and yet still accumulates VLCFA (23,30). Thus, the XALD and Vlcs mouse models demonstrate that VLCFA β-oxidation activity, while dependent on peroxisomal VLCS activity, does not determine VLCFA levels.

In the double knockout mouse, VLCFA levels are not increased beyond XALD mouse levels and VLCS and VLCFA β-oxidation activities are not further decreased beyond Vlcs mouse levels (Fig. 6). The biochemical characteristics of the two mice are not augmented but appear to be simply additive. We interpret these results to mean that Abcd1 and Vlcs do not interact and do not operate within the same metabolic pathways.

The combined absence of functional *Abcd1* and *Vlcs* genes in the double knockout mouse also does not produce a cerebral phenotype as none of the manifestations of childhood cerebral X-ALD—loss of sight, hearing, motor control, breathing and early death—are observed. XALD/Vlcs mice have normal litter sizes when compared with wild-type mice, so it is unlikely that embryonic lethality prevents an observation of a severe X-ALD phenotype. At an advanced age the X-ALD mouse displays some symptoms associated with adrenomyeloneuropathy (AMN) (27) and the XALD/Vlcs mouse models the metabolic and biochemical abnormalities described in human X-ALD fibroblasts, yet neither of these mice develop an X-ALD-like disease.

The X-ALD/Vlcs mouse may be a better model of late-stage AMN than the XALD mouse but it has not yet been examined for this possibility due to its age at the time of this writing. We believe this to be unlikely since there are no augmentations to the biochemistry of the double knockout to indicate that a more severe or an earlier phenotype will result.

These observations raise the following question: what is the source of VLCFA in X-ALD if not from decreased VLCFA β-oxidation? There is evidence that a significant fraction of VLCFA accumulating in X-ALD results from an increase in VLCFA synthesis, rather than a decrease in degradation. Oleate (C18:1), which has been shown to lower the VLCFA level in X-ALD fibroblasts by inhibiting the elongation of saturated fatty acids (31), and erucate (C22:1) are components of Lorenzo's Oil, a dietary supplement of 4:1 glycerol trioleate:glycerol trierucate that normalizes plasma levels of VLCFA in X-ALD patients (32). Further evidence for a synthetic source of VLCFA in X-ALD comes from Moser *et al.* (1,33), who measured the deuterium enrichment in brain VLCFA from a terminally ill X-ALD patient fed heavy water for 196 days prior to death. Significant amounts of label were detected in post-mortem brain VLCFA indicating that the source of these VLCFA was endogenous synthesis.

Fatty acid elongation, which requires acyl-CoA synthetase activity, occurs on microsomes where the majority of VLCS activity and Vlcs protein are found. If microsomal Vlcs is required for the elongation of saturated fatty acids to synthesize VLCFA, then the XALD/Vlcs mouse would not have been able to accumulate VLCFA. However, VLCFA remain high in the XALD/Vlcs double knockout mouse (Fig. 6C), indicating that microsomal Vlcs does not play a significant role in Abcd1-dependent VLCFA synthesis.

How mutations in ABCD1 may affect the microsomal fatty acid elongation system to increase VLCFA levels is not clear. Even if the source of VLCFA was known, a definitive link between VLCFA accumulation and X-ALD pathogenesis has not been established as the function of ABCD1 and the cause of X-ALD pathogenesis remain obscure. There are suggestions of a mitochondria/peroxisome interaction that may be disrupted by mutations in ABCD1 and it could be this interaction, rather than VLCFA accumulation, that is central to X-ALD pathology (30).

In summary, the Vlcs mouse generated here replicates both the decreased peroxisomal VLCS activity and the decreased VLCFA β-oxidation seen in X-ALD human fibroblasts. However, there is no accumulation of VLCFA in Vlcs mouse tissues and no severe neurological phenotype. The combination deficient Vlcs and Abcd1 genes in a double knockout mouse does not aggravate the XALD phenotype, nor does it result in an amplification of the biochemical abnormalities of the individual mice. We conclude that (1) VLCFA levels are not determined by peroxisomal VLCFA β-oxidation and that the accumulation seen in the XALD mouse and perhaps in X-ALD patients is due to effects on other VLCFA metabolic pathways, (2) that severe X-ALD phenotypes are not a result of decreased peroxisomal VLCS activity or decreased VLCFA β-oxidation and (3) that the ABCD1 gene has nothing to do with VLCFA β-oxidation and future X-ALD therapies should be evaluated on their effects on VLCFA levels not VLCFA β-oxidation.

MATERIALS AND METHODS

Disruption construct

Genomic sequences 5′ and 3′ of exon 3 were amplified from a 129Svev mouse strain genomic BAC clone known to contain the mouse *Vlcs* gene (Genome Systems, Inc., Palo Alto, CA, USA) using the following primers: 5′F2 (5′-CCGCCTCGAGGAAGCTGTGGAGGAGGCTCT-3′), 5′R (5′-CCGCCTCGAGGATTGATGGTTGCCGCTTT-3′), 3′F (5′-CGGGATCCCCACAATGCCCCTGTACCA-3′), and 3′R (5′-CGGGATCCGTACCGGAGCAGTTCACCAAT-3′). 5′F2 and 5′R have *Xho*I sites, and 3′F and 3′R have *Sal*I sites engineered into their 5′ ends (underlined). Thirty-six cycles of

amplification were performed with 30 s of denaturing at 95°C, 1 min of annealing at 61°C, and 5 min of synthesis at 68°C using a polymerase for long-range PCR (Roche). DNA fragments were gel purified and cloned into the vector pTA (Invitrogen, Carlsbad, CA, USA). These plasmids were restricted with *Xho*I and *Sal*I to release the inserts and these inserts were sequentially cloned into a vector containing a neomycin-resistance cassette, pMCneo1 (Invitrogen). The 5′ *Xho*I fragment was cloned upstream of the neomycin cassette in pMCneo1 into a *Xho*I site in the same orientation as the Neo cassette. The *Sal*I fragment was cloned into a *Sal*I site immediately 3′ of the Neo cassette of pMCneo1. After confirming the clone orientation by restriction enzyme digestion and DNA sequencing this plasmid was linearized with *Hind* III, phenol–chloroform extracted, precipitated with ethanol and dried. DNA was resuspended in endotoxin-free TE buffer and used for transfection of ES cells.

ES cell culture and transfection

Mouse embryonic stem cells (ES cells) from mouse line J1 129Svev were a gift from R. Reeves (Department of Physiology, Johns Hopkins Medical Institutions). This cell line had been employed previously to generate the X-ALD knockout mouse (34). As previously described, these cells were cultured at 37°C, 5% CO_2 in humid air on a layer of mitotically inactive neomycin-resistant mouse embryonic fibroblast feeder cells (35,36) (gift of A. Lawler, Department of Gynecology and Obstetrics, Johns Hopkins Medical Institutions). Fifty micrograms of linearized construct DNA in endotoxin-free TE buffer (1 µg/µl) were added to 2.5×10^7 cells/0.8 ml, electroporated in a GIBCO Cell Porator at 330 µF, 400 V and selected in 400 µg/ml G418. Homologous recombinant G418-resistant colonies were identified using southern blot analysis of *Hind*III restricted genomic DNA and a probe upstream of *Vlcs* exon 2. This 477 bp probe was generated by PCR with these primers: R23inv (5′-GGGGTAATGGCATATCCCTTTC-3′) and R20 (5′-CATGCCTTGCTGTCTTGTAGAG-3′). A 6 kb *Hind*III band represented a wild-type *Vlcs* allele and a 7 kb band indicated the presence of a disrupted *Vlcs* allele.

Colonies positive for homologous recombination were subjected to a karyotype analysis (Dr Clara Moore, Prenatal Cytogenetics Laboratory, Department of Gynecology and Obstetrics, Johns Hopkins Medical Institutions) and normal lines were injected into C57BL/6 embryos for chimera production. Germline-transmitting chimeras were crossed to 129svev mice to generate heterozygotes and these heterozygotes were crossed to each other to generate homozygous Vlcs knockout mice on a pure 129 genetic background, since germcells carrying the Vlcs knockout allele would be derived from the J1 129svev line. Four independent Vlcs knockout mouse lines were generated from four different clones and behaved similarly in all assays.

Animals

Wild-type 129Svev mice were obtained from Taconic Inc. (Germantown, NY, USA) and housed in the facility at the Johns Hopkins School of Medicine. XALD and Vlcs mice have been maintained in this facility as pure breeding lines since they were established (26). Double knockout XALD/Vlcs mice were derived by first generating double heterozygotes from homozygous Abcd1 females (XALD mice) and homozygous Vlcs males (Vlcs mice). Double heterozygotes from this cross were brother/sister mated to produce double homozygous females and *Abcd1* hemizygous/*Vlcs* homozygous males. These mice occurred, as expected, approximately once in every eight pups. Once double knockout genotypes were verified by PCR double homozygotes were bred to each other to establish the line. This line is true breeding as genotypes remained constant over two generations.

Animals were housed under controlled conditions between 22 and 27°C on a 12 h light–dark cycle with free access to food and water. Procedures involving animals and their care were conducted in conformity with the institutional guidelines that are in compliance with national and international laws and policies (EEC Council Directive 86/609, OJ L 358, 1 DEC.12,1987; NIH Guide for the Care and Use of Laboratory Animals, US National Research Council, 1996).

Genotyping

Abcd1 genotyping. *Abcd1* PCR genotyping has been described previously (26). Briefly, PCR primers Abcd1a (5′-ATGTGGTAGCCTTGCTG-3′) and Abcd1b (5′-CCTCAGAAGAACTCGTCAAG-3′) amplify the region of the mouse *Abcd1* locus that contains the disruption cassette. Wild-type allele PCR templates produce a 3.5 kb PCR product and *Abcd1* knockout allele templates produce a 4.5 kb PCR product.

Vlcs genotyping. Two PCR assays were performed per sample to determine the *Vlcs* genotype. The first set of primers, Vlcs KO C (5′-CTCCCTGCATTGGTGTGAGAGAATTTTG-3′) and Vlcs KO B (5′-TTAGTCAGATGCCAACCATAGGCAAGCT-3′), generate a 500 bp product from a wild-type *Vlcs* allele and a 1500 bp product from the *Vlcs* allele disrupted by a neomycin-resistance cassette. The second set of primers also uses Vlcs KO C as the forward primer but uses a primer within the neomycin-resistance cassette NeoR1 (5′-GAAGAACTCGTCAAGAAGGCG-3′) as the reverse primer. This primer pair generates a 1100 bp product from disrupted *Vlcs* alleles and nothing from wild-type *Vlcs* alleles. Both PCR assays use the same conditions: 0.2 g of genomic DNA, 1.8 mM $MgCl_2$, 0.5 mM dNTPs, 0.5 mM each primer, 0.5 U *Taq* polymerase (Promega, Madison, WI, USA), and 1× PCR buffer (Promega) in a 50 µl reaction. Reactions were set up on ice and introduced to a preheated 95°C PCR block. After 1 min of denaturation, samples were subjected to 36 cycles of 95°C for 15 s, 57°C for 15 s, 72°C for 2 min. A final 5 min 72°C extension step ended the PCR cycle. Samples that had been genotyped previously by Southern blot analysis were used as positive and negative controls.

Western blot analysis

Western blots were performed on tissue homogenates from 6–8-week-old mice and density gradient fractions as described previously (23). Rabbit IgG anti-human PEX14 antibodies were a generous gift of S. Gould (Departments of Biological

Chemistry and Cell Biology and Anatomy, Johns Hopkins Medical Institutions) and were used at a 1/100 dilution to detect mouse Pex14 protein in peroxisomal membranes (37). Rabbit IgG anti-mouse Vlcs antibodies were produced (see below) and used at a 1/1000 dilution. A chemiluminescent detection system was used to develop the blot and blots were exposed to film for varying times from 30 s to 5 min.

Antibody production

A fusion protein of maltose binding protein, MBP, and the C-terminal 214 amino acids of Vlcs was created using a bacterial expression vector containing MBP cDNA (New England Biolabs, Beverly, MA, USA) and mouse *Vlcs* cDNA. Protein synthesis was induced in BL21 DE3 *E. coli* by addition of 0.1 mM isopropyl-beta-D-thiogalactopyranoside (IPTG) and incubation for 4 h at 37°C. *E. coli* protein extracts were solubilized in 0.4 mM NaCl, purified over a maltose column and concentrated to 1 mg/ml. One-hundred micrograms of this concentrate were mixed with Freud's complete adjuvant and inoculated into New Zealand White rabbits. A 50 µg boost was given at 2, 3 and 7 weeks (Cocalico Biologicals Inc., Reamstown, PA, USA). Sera from week 8 was affinity purified against a glutathione-*S*-transferase (GST) (Promega, Madison, WI, USA) Vlcs fusion protein, in which the C-terminal 263 amino acids of Vlcs are fused to GST. The purified sera were concentrated and used at 1/200 dilution for in immunofluorescence studies and 1/500 dilution for western blot analyses.

Histology

Freshly dissected mouse organs from 6–8-week-old males were flash frozen in isopentane that had been cooled in liquid nitrogen. Tissues were stored at −80°C for less than 1 month. Five to 10 µm sections were cut on a cryotome at −20°C and collected on poly-L-lysine-coated glass slides. Sections were air-dried, fixed in a 3% solution of formaldehyde for 30 min, stained with hematoxylin and eosin and mounted.

Acyl-CoA synthetase assays

Tissues from mouse organs were homogenized in 10 volumes of cold STE buffer (250 mM sucrose, 10 mM Tris–HCl pH 7.5, 1 mM EDTA) with a Potter–Elvehjem homogenizer. Debris and nuclei were removed by centrifugation at 3000*g* for 30 s. The supernatant protein concentrations were measured via the method of Lowry (38) and adjusted to 2 mg/ml with STE buffer. Samples were stored at −80°C for at least 24 h and up to several months before assaying. Length of time in storage did not alter activity levels.

Acyl-CoA synthetase activity was measured by the method previously described (39). An aliquot of post-nuclear supernatant containing 20–40 µg of protein was added to a 250 µl reaction containing 20 µM [1-^{14}C] lignoceric acid (C24:0, Moravek Biochemicals, Brea, CA, USA ~20 000 dpm/nmol). Duplicate assays were performed for each measurement and the average value reported as nmols of CoA derivative generated in 20 min per mg protein.

C24:0 β-oxidation

Frozen post-nuclear supernatants prepared for synthetase assays were also used to measure β-oxidation activity as previously described (40). Assays contained 100–200 µg protein along with 20 µM [1-^{14}C] lignoceric acid. Duplicate reactions were measured for each sample and activity was expressed as nmol of radiolabeled acetate made in 1 h per mg protein.

Measurement of fatty acids

Tissues from three mice of each genotype, wild type, *Vlcs*, XALD and XALD/Vlcs, were dissected and weighed. Two hundred milligrams of tissue from liver, kidney or brain were frozen and stored at −80°C for future analysis or immediately minced and solubilized in 4 ml of chloroform: methanol (2:1, v/v) with a ground glass v-bottom test tube and glass pestle. Two ml of chloroform:methanol (1:1, v/v) were added to each sample and allowed to sit for 1 h at room temperature. Insoluble material was removed by centrifugation at 500g for 10 min at room temperature; supernatants were dried under nitrogen and weighed for total lipid weight (about 0.2 g). Lipids were resuspended in chloroform or hexane to a concentration of 0.1 g/ml. Two milliliters of hexane or chloroform containing 0.2 g of tissue total lipid were dried under nitrogen and resuspended in 1.25 ml of methanol:methylene chloride (3:1, v/v) with BHT (50 ng/l) and methyl ester derivatives were made and quantified by gas chromatography as previously described (41).

REFERENCES

1. Moser, H.W., Smith, K.D., Watkins, P.A., Powers, J.M. and Moser, A.B. (2000) X-linked adrenoleukodystrophy. In Scriver, C.R., Sly, W.S., Childs, B., Beaudet, A.L., Valle, D., Kinzler, K.W. and Vogelstein, B. (eds), *The Metabolic and Molecular Bases of Inherited Disease*, 8th ed. McGraw Hill, New York, Vol. III, pp. 3257–3301.
2. Singh, I., Moser, A.E., Moser, H.W. and Kishimoto, Y. (1984) Adrenoleukodystrophy: impaired oxidation of very long chain fatty acids in white blood cells, cultured skin fibroblasts, and amniocytes. *Pediatr. Res.*, **18**, 286–290.
3. Rizzo, W.B., Avigan, J., Chemke, J. and Schulman, J.D. (1984) Adrenoleukodystrophy: very long-chain fatty acid metabolism in fibroblasts. *Neurology*, **34**, 163–169.
4. Singh, H., Derwas, N. and Poulos, A. (1987) Beta-oxidation of very-long-chain fatty acids and their coenzyme A derivatives by human skin fibroblasts. *Arch. Biochem. Biophys.*, **254**, 526–533.
5. Wanders, R.J., van Roermund, C.W., van Wijland, M.J., Heikoop, J., Schutgens, R.B., Schram, A.W., Tager, J.M., van den Bosch, H., Poll-The, B.T., Saudubray, J.M. *et al.* (1987) Peroxisomal very long-chain fatty acid beta-oxidation in human skin fibroblasts: activity in Zellweger syndrome and other peroxisomal disorders. *Clin. Chim. Acta*, **166**, 255–263.
6. Hashmi, M., Stanley, W. and Singh, I. (1986) Lignoceroyl-CoASH ligase: enzyme defect in fatty acid beta-oxidation system in X-linked childhood adrenoleukodystrophy. *FEBS Lett.*, **196**, 247–250.
7. Lazo, O., Contreras, M., Hashmi, M., Stanley, W., Irazu, C. and Singh, I. (1988) Peroxisomal lignoceroyl-CoA ligase deficiency in childhood adrenoleukodystrophy and adrenomyeloneuropathy. *Proc. Natl Acad. Sci. USA*, **85**, 7647–7651.
8. Wanders, R.J., van Roermund, C.W., Schutgens, R.B., van den Bosch, H. and Tager, J.M. (1988) Impaired ability of peroxisomes to activate very-long-chain fatty acids in X-linked adrenoleukodystrophy. *Lancet*, **2**, 170.

9. Mosser, J., Douar, A.M., Sarde, C.O., Kioschis, P., Feil, R., Moser, H., Poustka, A.M., Mandel, J.L. and Aubourg, P. (1993) Putative X-linked adrenoleukodystrophy gene shares unexpected homology with ABC transporters. *Nature*, **361**, 726–730.
10. Cartier, N., Lopez, J., Moullier, P., Rocchiccioli, F., Rolland, M.O., Jorge, P., Mosser, J., Mandel, J.L., Bougneres, P.F. and Danos, O. *et al.* (1995) Retroviral-mediated gene transfer corrects very-long-chain fatty acid metabolism in adrenoleukodystrophy fibroblasts. *Proc. Natl Acad. Sci. USA*, **92**, 1674–1678.
11. Shinnoh, N., Yamada, T., Yoshimura, T., Furuya, H., Yoshida, Y., Suzuki, Y., Shimozawa, N., Orii, T. and Kobayashi, T. (1995) Adrenoleukodystrophy: the restoration of peroxisomal beta-oxidation by transfection of normal cDNA. *Biochem. Biophys. Res. Commun.*, **210**, 830–836.
12. Braiterman, L.T., Zheng, S., Watkins, P.A., Geraghty, M.T., Johnson, G., McGuinness, M.C., Moser, A.B. and Smith, K.D. (1998) Suppression of peroxisomal membrane protein defects by peroxisomal ATP binding cassette (ABC) proteins. *Hum. Mol. Genet.*, **7**, 239–247.
13. Uchida, Y., Kondo, N., Orii, T. and Hashimoto, T. (1996) Purification and properties of rat liver peroxisomal very-long-chain acyl-CoA synthetase. *J. Biochem. (Tokyo)*, **119**, 565–571.
14. Uchiyama, A., Aoyama, T., Kamijo, K., Uchida, Y., Kondo, N., Orii, T. and Hashimoto, T. (1996) Molecular cloning of cDNA encoding rat very long-chain acyl-CoA synthetase. *J. Biol. Chem.*, **271**, 30360–30365.
15. Watkins, P.A., Lu, J.F., Braiterman, L.T., Steinberg, S.J. and Smith, K.D. (2000) Disruption of a yeast very-long-chain acyl-CoA synthetase gene simulates the cellular phenotype of X-linked adrenoleukodystrophy. *Cell. Biochem. Biophys.*, **32** (Spring), 333–337.
16. Berger, J., Truppe, C., Neumann, H. and Forss-Petter, S. (1998) A novel relative of the very-long-chain acyl-CoA synthetase and fatty acid transporter protein genes with a distinct expression pattern. *Biochem. Biophys. Res. Commun.*, **247**, 255–260.
17. Berger, J., Truppe, C., Neumann, H. and Forss-Petter, S. (1998) cDNA cloning and mRNA distribution of a mouse very long-chain acyl-CoA synthetase. *FEBS Lett.*, **425**, 305–309.
18. Hirsch, D., Stahl, A. and Lodish, H.F. (1998) A family of fatty acid transporters conserved from mycobacterium to man. *Proc. Natl Acad. Sci. USA*, **95**, 8625–8629.
19. Coe, N.R., Smith, A.J., Frohnert, B.I., Watkins, P.A. and Bernlohr, D.A. (1999) The fatty acid transport protein (FATP1) is a very long chain acyl-CoA synthetase. *J. Biol. Chem.*, **274**, 36300–36304.
20. Steinberg, S.J., Morgenthaler, J., Heinzer, A.K., Smith, K.D. and Watkins, P.A. (2000) Very long-chain acyl-CoA synthetases. Human 'bubblegum' represents a new family of proteins capable of activating very long-chain fatty acids. *J. Biol. Chem.*, **275**, 35162–35169.
21. Steinberg, S.J., Mihalik, S.J., Kim, D.G., Cuebas, D.A. and Watkins, P.A. (2000) The human liver-specific homolog of very long-chain acyl-CoA synthetase is cholate:CoA ligase. *J. Biol. Chem.*, **275**, 15605–15608.
22. Steinberg, S.J., Kemp, S., Braiterman, L.T. and Watkins, P.A. (1999) Role of very-long-chain acyl-coenzyme A synthetase in X-linked adrenoleukodystrophy. *Ann. Neurol.*, **46**, 409–412.
23. Heinzer, A.K., Kemp, S., Lu, J.F., Watkins, P.A. and Smith, K.D. (2002) Mouse very long-chain acyl-CoA synthetase in X-linked adrenoleukodystrophy. *J. Biol. Chem.*, **277**, 28765–28773.
24. Forss-Petter, S., Werner, H., Berger, J., Lassmann, H., Molzer, B., Schwab, M.H., Bernheimer, H., Zimmermann, F. and Nave, K.A. (1997) Targeted inactivation of the X-linked adrenoleukodystrophy gene in mice. *J. Neurosci. Res.*, **50**, 829–843.
25. Kobayashi, T., Shinnoh, N., Kondo, A. and Yamada, T. (1997) Adrenoleukodystrophy protein-deficient mice represent abnormality of very long chain fatty acid metabolism. *Biochem. Biophys. Res. Commun.*, **232**, 631–636.
26. Lu, J.F., Lawler, A.M., Watkins, P.A., Powers, J.M., Moser, A.B., Moser, H.W. and Smith, K.D. (1997) A mouse model for X-linked adrenoleukodystrophy. *Proc. Natl Acad. Sci. USA*, **94**, 9366–9371.
27. Pujol, A., Hindelang, C., Callizot, N., Bartsch, U., Schachner, M. and Mandel, J.L. (2002) Late onset neurological phenotype of the X-ALD gene inactivation in mice: a mouse model for adrenomyeloneuropathy. *Hum. Mol. Genet.*, **11**, 499–505.
28. Bezman, L., Moser, A.B., Raymond, G.V., Rinaldo, P., Watkins, P.A., Smith, K.D., Kass, N.E. and Moser, H.W. (2001) Adrenoleukodystrophy: incidence, new mutation rate, and results of extended family screening. *Ann. Neurol.*, **49**, 512–517.
29. McGuinness, M.C., Lu, J.F., Zhang, H.P., Dong, G.X., Heinzer, A.K., Watkins, P.A., Powers, J. and Smith, K.D. (2003) Role of ALDP (ABCD1) and mitochondria in X-linked adrenoleukodystrophy. *Mol. Cell. Biol.*, **23**, 744–753.
30. McGuinness, M.C., Zhang, H.P. and Smith, K.D. (2001) Evaluation of pharmacological induction of fatty acid beta-oxidation in X-linked adrenoleukodystrophy. *Mol. Genet. Metab.*, **74**, 256–263.
31. Rizzo, W.B., Watkins, P.A., Phillips, M.W., Cranin, D., Campbell, B. and Avigan, J. (1986) Adrenoleukodystrophy: oleic acid lowers fibroblast saturated C22-26 fatty acids. *Neurology*, **36**, 357–361.
32. Rizzo, W.B., Leshner, R.T., Odone, A., Dammann, A.L., Craft, D.A., Jensen, M.E., Jennings, S.S., Davis, S., Jaitly, R. and Sgro, J.A. (1989) Dietary erucic acid therapy for X-linked adrenoleukodystrophy. *Neurology*, **39**, 1415–1422.
33. Moser, H.W., Pallante, S.L., Moser, A.E., Rizzo, W.B., Schulman, J.D. and Fenselau, C. (1983) Adrenoleukodystrophy: origin of very long chain fatty acids and therapy. *Pediatr. Res.*, **17**, 293a.
34. Li, E., Bestor, T.H. and Jaenisch, R. (1992) Targeted mutation of the DNA methyltransferase gene results in embryonic lethality. *Cell*, **69**, 915–926.
35. Axelrod, H.R. (1984) Embryonic stem cell lines derived from blastocysts by a simplified technique. *Dev. Biol.*, **101**, 225–228.
36. Doetschman, T., Williams, P. and Maeda, N. (1988) Establishment of hamster blastocyst-derived embryonic stem (ES) cells. *Dev. Biol.*, **127**, 224–227.
37. Sacksteder, K.A., Jones, J.M., South, S.T., Li, X., Liu, Y. and Gould, S.J. (2000) PEX19 binds multiple peroxisomal membrane proteins, is predominantly cytoplasmic, and is required for peroxisome membrane synthesis. *J. Cell. Biol.*, **148**, 931–944.
38. Lowry, O.H., Rosebrough, J.N., Farr, A.L. and Randall, R.J. (1951) Protein measurements with the Folin reagent. *J. Biol. Chem.*, **193**, 265–275.
39. Watkins, P.A., Ferrell, E.V., Jr., Pedersen, J.I. and Hoefler, G. (1991) Peroxisomal fatty acid beta-oxidation in HepG2 cells. *Arch. Biochem. Biophys.*, **289**, 329–336.
40. Hoefler, G., Hoefler, S., Watkins, P.A., Chen, W.W., Moser, A., Baldwin, V., McGillivary, B., Charrow, J., Friedman, J.M., Rutledge, L. *et al.* (1988) Biochemical abnormalities in rhizomelic chondrodysplasia punctata. *J. Pediatr.*, **112**, 726–733.
41. Rasmussen, M., Moser, A.B., Borel, J., Khangoora, S. and Moser, H.W. (1994) Brain, liver, and adipose tissue erucic and very long chain fatty acid levels in adrenoleukodystrophy patients treated with glyceryl trierucate and trioleate oils (Lorenzo's oil). *Neurochem. Res.*, **19**, 1073–1082.